PROCEEDINGS, 51st Workshop on Geothermal Reservoir Engineering
Stanford University, Stanford, California, February 9-11, 2026
SGP-TR-230

Application of Neural Operators for Reactive Transport Modeling of CO_2 Reinjection into Geothermal Reservoirs

Tao Wang[1], James W. Patterson[2,3], David J. Byrne[3], and Hewei Tang[1]

[1]Department of Petroleum & Geosystems Engineering, UT Austin, Austin, Texas 78712-1585, USA

[2]Geothermal Energy & Geofluids, Institute of Geophysics, NO F 61.1, Sonneggstrasse 5, CH-8092 Zurich Switzerland

[3]New Zealand Institute of Earth Science, 114 Karetoto Road, Wairakei, Taupō 3377, New Zealand

tao.wang@utexas.edu, james.patterson@eaps.ethz.ch, d.byrne@gns.cri.nz, hewei.tang@austin.utexas.edu

Keywords: neural operators, deep learning, geothermal energy, reactive transport, silica scaling

ABSTRACT

Emission of dissolved non-condensable CO_2 is a major contributor to the geothermal carbon footprint of conventional geothermal energy development, and reinjection of CO_2 with produced brine is a technique to reduce carbon emission intensities. A previous study has found that the addition of CO_2 can significantly reduce the rate of silica precipitation in greywacke (a typical Taupo Volcanic Zone reservoir rock) sand packs. Silica precipitation is responsible for the injectivity decline of conventional geothermal wells. In this study, we propose to leverage neural operators to model geothermal reactive transport. Neural operators are designed to learn the solution operators of partial differential equations (PDEs) by mapping between infinite-dimensional function spaces. Fourier neural operators (FNOs) have good potential to approximate complex PDE systems using the Fourier transform. Meanwhile, the integration of trained neural operator surrogate models into an inversion workflow will significantly speed up the process. In this study, FNO surrogate models are trained to model reactive transport of CO_2 reinjection column experiments and to replace a conventional reactive transport numerical solver (PFLOTRAN) in a PESTPP-IES inversion workflow for estimation of geochemical parameters. The trained FNO surrogates can predict the temporal outlet silica concentrations, calcium concentrations, and pH values of the complex reactive transport system with high accuracy (R^2 scores up to 0.9998) and superior time efficiency (95.6% faster than PFLOTRAN). With the implementation of FNO surrogates, the time cost of the inversion workflow has reduced by 34.5%, while achieving almost identical results as the workflow with PFLOTRAN. The investigation demonstrated the speedup advantages of implementing FNO surrogates against conventional reactive transport solvers in inverse modeling. The study will be instructive to employ neural operators to model reactive transport and estimate reactive transport parameters in geothermal applications.

1. INTRODUCTION

Over the past decade, the development of geothermal energy has attracted much attention from the scientific and engineering communities due to its potential to reduce energy carbon footprint. During a conventional geothermal application, formation brine is circulated as the working fluid to extract thermal energy from geothermal reservoirs. Studies have demonstrated silica scaling is common in high enthalpy geothermal reservoirs when rapid fluid-cooling happens (Hirtz, 2016; Heuvel and Daniela, 2018; Hassani and Zheng, 2025). This scaling reduces the fluid flow rate and may also clog the fluid paths, which is one of the major challenges for conventional geothermal applications (Hassani and Zheng, 2025). In New Zealand Taupo Volcanic Zone, the exploitation of geothermal energy by-produces CO_2, a main contributing greenhouse gas for global warming. To reduce the carbon emission intensity associated with geothermal development, CO_2 reinjection with produced brine is proposed. During initial investigations, results from numerical simulations and laboratory experiments confirm that the reinjection of CO_2 with brine will significantly inhibit silica precipitation in geothermal reservoirs (Byrne et. al, 2023). These findings will help future geothermal applications to operate at high flow rates over extended life spans while minimizing carbon footprint.

CO_2 reinjection with brine for geothermal applications is a reactive transport problem. During the process, reinjected brine reacts with host rock around the injector well, changing the chemical composition of the fluid and causing silica either to precipitate or dissolve. These geochemical reactions subsequently change matrix permeability and porosity due to minerals' dissolution or precipitation. To fully understand geothermal reactive transport, numerical simulators such as TOUGHREACT or PFLOTRAN are employed to simulate the process. The computation cost of modeling geothermal reactive transport can be prohibitively high (Wang et. al, 2019). This computational bottleneck is even more pronounced in workflows of inversion, sensitivity analysis, and uncertainty quantification, where up to thousands of forward simulations are required. This has inspired the concept of deploying fast and accurate surrogate models in these workflows over the past decades. One category of surrogate models belongs to data-driven machine learning approaches. These models are trained with synthetic datasets from numerical solvers and then integrated into workflows to replace conventional numerical solvers and significantly speed up these workflows.

Neural operator learning, as a newly emerging data-driven deep learning approach, has exhibited great potential in subsurface surrogate modeling. Li et.al (2020) introduce Fourier neural operator, or FNO, to approximate the solution operator of parametric partial differential equations (PDEs). Over the years, FNOs have been applied to subsurface surrogate modeling in multiple directions. Wen et. al (2023) propose a hierarchical nested FNO structure to model high-resolution dynamic 3D CO_2 storage modeling at a basin scale, and the

framework achieves 700,000 times speedup for flow prediction compared to existing methods. Tang et.al (2024) propose to employ a multi-fidelity FNO to solve large-scale geological carbon storage problems with more affordable multi-fidelity training datasets. With resolution-invariant capacity of FNOs, they successfully leverage the transfer learning procedure to give accurate predictions with very limited high-resolution training datasets. Guo et. al (2024) propose an RGA-FNO framework in which the reduced geostatistical approach (RGA) with an FNO surrogate model for inverse modeling of hydraulic tomography. Their results demonstrate that great potential for neural operators like FNOs to play an important role in groundwater modeling, especially in inverse modeling.

In this paper, Fourier neural operator is employed to model reactive transport in a geothermal context. Of particular interest is to integrate the FNO surrogates into PESTPP-IES inversion workflow to estimate geochemical parameters that governs the reactive transport process and to history match corresponding laboratory results from the New Zealand Institute of Earth Science. With these goals, comparisons of predictions from FNO surrogates against reference values from PFLOTRAN simulations are performed to quantify the accuracy of FNO surrogates. Then FNO surrogates are then integrated into the same inversion workflow to compete with PFLOTRAN on history matching accuracy and time efficiency.

2. METHODS

In the section, we briefly present the problem of interest by including the governing equations, laboratory investigation, and numerical simulation in problem setting. Then, we introduce the methods, i.e. Fourier neural operator and PESTPP-IES employed for our proposed tasks.

2.1 Problem Setting

2.1.1 Governing Equations

CO_2 reinjection with produced brine from a geothermal reservoir can be modeled as a multiphase reactive transport problem. It is assumed that no active gas phase is present during the reactive transport process. The reinjected CO_2 dissolves in the brine, transports with the flow circulation, and participates in geochemical reactions. With the ongoing geochemical reactions, the minerals' volume fractions will either increase or decrease, which is subject to the conservation of elements in the system. Subsequently, the matrix permeability and porosity are also updated with respect to either dissolution or precipitation of reactive minerals. The mass conservation equation for a set of independent aqueous primary species is expressed as:

$$\frac{\partial}{\partial t}\left(\phi \sum_\alpha s_\alpha \Psi_j^\alpha\right) + \nabla \cdot \sum_\alpha \Omega_j^\alpha = Q_j - \sum_m v_{jm} I_m \tag{1}$$

where ϕ is the matrix porosity, s_α is the saturation of phase α, Ψ_j^α is the total concentration of j^{th} primary species in phase α , Ω_j^α is the total flux of j^{th} primary species with respect to phase α, Q_j is the sink or source term for j^{th} primary species, v_{jm} is the number of moles of primary species m in one mole of secondary species j, and I_m is the reaction rate of m^{th} mineral.

The Darcy velocity q_α for phase α is given by:

$$q_\alpha = -\frac{k k_\alpha}{\mu_\alpha} \nabla (p_\alpha - \rho_\alpha g z) \tag{2}$$

where k is the absolute permeability of the matrix, k_α is the relative permeability of phase α, μ_α is the viscosity of phase α, p_α is the pressure of phase α, ρ_α is the density of phase α, g is the gravitational acceleration, and z is the elevation.

The matrix porosity is updated with:

$$\frac{\partial \phi_m}{\partial t} = \overline{V_m} I_m \tag{3}$$

$$\phi = 1 - \sum_m \phi_m \tag{4}$$

where ϕ_m is the mineral volume fraction, $\overline{V_m}$ is mineral molar volume, and I_m is the reaction rate.

The matrix permeability is updated with:

$$k = k_0 f \tag{5}$$

$$f = \begin{cases} \left(\frac{\phi - \phi_c}{\phi_0 - \phi_c}\right)^n, & \phi > \phi_c \\ f_{min}, & \phi \le \phi_c \end{cases} \tag{6}$$

where k is the matrix permeability, k_0 is the initial matrix permeability, f is the permeability scale factor, ϕ is the current matrix porosity, ϕ_c is the critical porosity below which the matrix permeability is assumed to be constant with scale factor f_{min}, ϕ_0 is the initial matrix porosity, n is the exponent reflecting the surface to volume ratio, and f_{min} is the minimal scale factor when $\phi \le \phi_c$.

2.1.2 Laboratory Investigation

The New Zealand Institute of Earth Science has conducted laboratory investigations on CO_2 reinjection with produced brine using greywacke (a typical Taupo Volcanic Zone reservoir rock) sand packs (Byrne et. al, 2023). In the four CO_2 reinjection experiments, high-PT flow-through reactors under geochemical conditions relevant to New Zealand geothermal reservoirs are employed with varying concentrations of added CO_2. The experimental investigations run 31 days at 150 °C and 7.5 MPa with a constant flow rate of 5 ml/hour. The effluent is also sampled daily to perform major element analysis. A summary of the four experimental materials and fluids is given in **Table 1**.

Table 1: Materials and fluids for CO_2 reinjection experiments SAE_1-4.

Experiments	Materials	Fluids
SAE_1	greywacke	unmodified brine
SAE_2	greywacke + 1.5 wt.% calcite	unmodified brine
SAE_3	greywacke + 1.5 wt.% calcite	unmodified brine + 2000 ppm CO_2
SAE_4	greywacke + 1.5 wt.% calcite	unmodified brine + 600 ppm CO_2

2.1.3 Numerical Simulation

The GIRT (Global Implicit Reactive Transport) module in PFLOTRAN (v6.0) is employed to build the geothermal reactive transport model. To model the laboratory experiments, the grid is set to 1D as shown in **Figure 1**. The same experimental conditions, including fluid compositions, flow rate, temperature, and pressure, are used for the simulations. The reporting time steps are set identical to laboratory experiments. The primary reactive minerals included in the simulations are calcite, quartz, albite, amorphous silica, and amorphous aluminous silica. The current selection of primary minerals is enough to capture the major geochemical reactions in the reactive transport system. Mineral kinetic parameters in this study are taken from Palandri and Kharaka (2004) and fixed, except for key parameters such as the dependence of amorphous aluminous silica or silica precipitation or dissolution on H^+ abundance. The precipitation or dissolution rates are also controlled by mineral specific surface areas, which may vary with ongoing of the geochemical process, as well as parameters controlling the relationship between surface area and volume fraction for each reactive primary mineral. The PFLOTRAN simulations are used to build a comprehensive synthetic dataset for training the FNO surrogates.

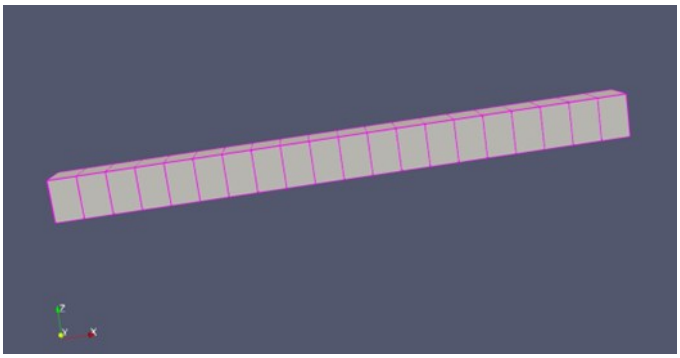

Figure 1: The 1D simulation setup for modeling geothermal reactive transport

2.2 Fourier Neural Operator

Neural Operators learn a mapping between two infinite-dimensional spaces from a finite collection of input-output pairs, which enables them to learn the solution operators of partial differential equations associated with subsurface processes. Solving geothermal reactive transport problems defined on a domain $D \subset R^d$ means finding a nonlinear mapping $\mathcal{G}^*$ from input function spaces $\mathcal{A} \subset R^{d_a}$ to output function spaces $\mathcal{U} \subset R^{d_u}$ that satisfies relevant governing equations. Fourier Neural Operator, $\mathcal{G}_\theta$, is applied to learn the solution mapping between $\boldsymbol{a}(x) \in \mathcal{A}$ and $\boldsymbol{u}(x) = \mathcal{G}^*(\boldsymbol{a}(x))$. In an FNO structure, the continuous input and output spaces on a domain $D \subset R^d$ are represented in Fourier space by using the Fourier transform, and the global convolution of the domain is achieved by the pointwise multiplication in the Fourier domain. The detailed model structure can be found in Li et.al (2020).

2.3 Inverse Modeling

In the proposed inversion workflows, realizations of parameter ensembles are iteratively updated through history matching experimental data using PESTPP-IES. PESTPP-IES was first introduced by White (2018), which is a direct implementation of the iterative ensemble smoother algorithm from Chen and Oliver (2013). Within each iteration, the PESTPP-IES algorithm combines the efficiency of the GLM (Gauss-Levenberg-Marquardt) algorithm to minimize a least-squares objective function in high-dimensional spaces with Monte Carlo. In our study, the method is used to constrain the uncertainties of kinetic parameters of mineral dissolution and precipitation in laboratory

experiments, and the parameters and ranges are given in **Table 2**. Daily effluent element measurements from SAE_1-4 are used for history matching, which include pH values, concentration of silica, and concentration of Ca^{2+}. The objective function summary or phi value for the PESTPP-IES inversion workflow is defined as:

$$\varphi = \sum_{i=1}^{N_{obs}} w_i^2 (d_i - m_i)^2 \quad (7)$$

where φ is the phi value, N_{obs} is the number of observations, w_i is the weight of observation i, d_i is the value of observation i, and m_i is the i^{th} simulation value.

Table 2: Summary of prior parameter ranges in inverse modeling.

parameters	ranges
SURFACE_AREA_VOL_FRAC_POWER for calcite	[4.0, 8.0]
SURFACE_AREA_VOL_FRAC_POWER for original calcite	[3.0, 9.0]
SURFACE_AREA_VOL_FRAC_POWER for SiO_2 (am) and alu-SiO_2 (am)	[0.1, 1.0]
alpha value for SiO_2 (am) and alu-SiO_2 (am)	[-1.25, -0.75]
specific area of calcite (m^2/m^3)	[10, 500]
specific area of calcite_slow (m^2/m^3)	[10, 100]
specific area of SiO_2 (am) (m^2/m^3)	[10, 500]
specific area of alu-SiO_2 (am) (m^2/m^3)	[10, 500]

3. RESULTS AND DISCUSSION

For building a comprehensive dataset for training FNO surrogates, 1,100 PFLOTRAN simulations are performed with geochemical parameters of reactive minerals, initial calcite volume fraction, and initial CO_2 concentration. These parameters are sampled with a Latin Hypercube sampling method to make inputs for running the simulations and training the FNO surrogates. In training the FNO surrogates, the comprehensive dataset is split into training (900 cases), validation (100 cases), and test (100 cases) datasets. Based on the split, A grid search method is leveraged to tune the hyperparameters for the FNO surrogates on pH, silica concentration, and Ca^{2+} concentration, and the tuned FNO surrogates are further evaluated with test dataset. Then, the trained FNO surrogates are integrated into the inversion workflow of PESTPP-IES to estimate the geochemical parameters as in the conventional workflow with numerical solver PFLOTRAN.

3.1 FNO Surrogates

In this part, the optimized model structures and training parameters after hyperparameter tuning using the grid search method for FNO surrogates are presented, as in **Table 3**. Here 4 hyperparameters are considered for the FNO surrogates which are the number of Fourier layers, modes, widths, and learning rates. Then we demonstrate the accuracy of FNO surrogates in predicting the silica concentration, pH, and Ca^{2+} concentration from the effluent, as shown in **Figure 2** to **4**. To construct the following plots the temporal reference and prediction in 100 test cases are flattened to make point-wise comparison.

Table 3: Summary of hyperparameters tuning for FNO surrogates.

species	Fourier-layers	modes	width	learning rate	No. of params	avg. relative L_2 loss per case		
						train	validate	test
SiO_2	6	4	48	0.01	158,305	0.0026	0.0052	0.0068
pH	4	12	64	0.005	452,353	0.0027	0.0047	0.0055
Ca^{2+}	4	4	48	0.005	107,329	0.0040	0.0073	0.0081

In general, the FNO surrogates with tuned hyperparameters demonstrate great ability to generalize from validation dataset to test dataset with a slight increase in the relative L_2 loss per case in test dataset. The cross plots of predictions and references also confirm that these FNO surrogates are very accurate, with R^2 values of 0.9974, 0.9997, and 0.9998 for test dataset of silica concentration, pH, and calcium

concentration, respectively. The average time for one PFLOTRAN simulation to build the dataset for training the FNO surrogates is 1.009 seconds due to the simplicity of the grids. While the average time cost for FNO surrogates to map from an input to outputs is 0.044 seconds. The FNO surrogates yield a 95.6% reduction in computational time compared to PFLOTRAN simulations. The good generalization, high accuracy, and fast speed of these FNO surrogates make them promising alternatives for forward modeling in PESTPP-IES inversion workflows.

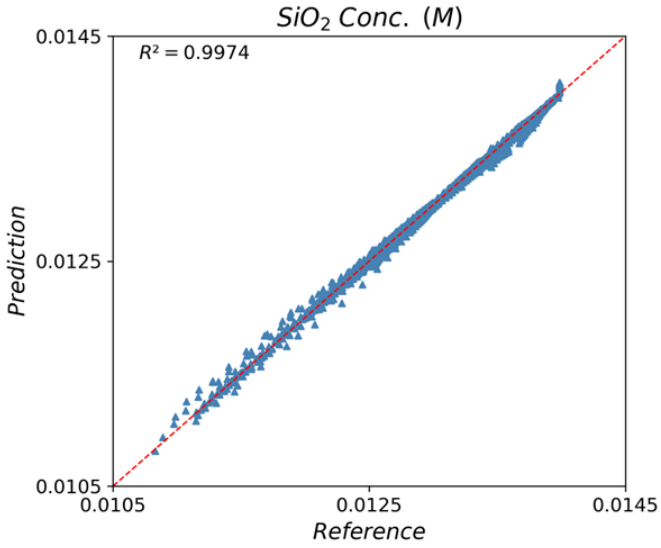

Figure 2: The predictions and references of silica concentration from test dataset (*M: mol/L*)

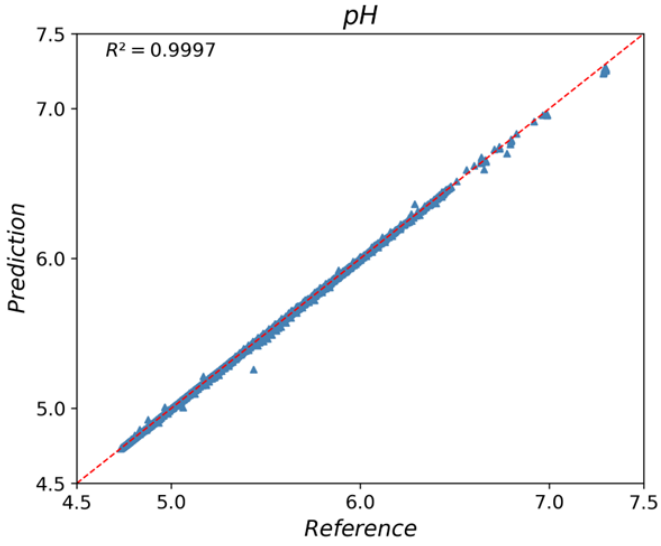

Figure 3: The predictions and references of pH from test dataset

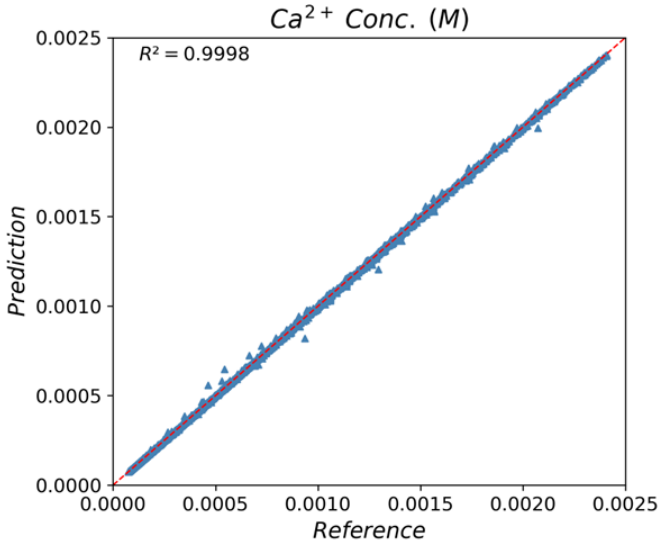

Figure 4: The predictions and references of Ca^{2+} concentration from test dataset (*M: mol/L*)

3.2 PESTPP-IES Inversion via FNO Surrogates

Two workflows are developed to update the uncertain parameter ranges using PESTPP-IES. One workflow relies on the conventional numerical solver PFLOTRAN, while the other workflow employs FNO surrogates. To make a fair comparison, the two workflows are set to have 55 realizations for 10 iterations and 15 iterations, and all other conditions are set identical. Evaluation of the two workflows involves comparing time cost, overall accuracy, and visualization of realizations. **Table 4** presents the results for the two inversion workflows.

The phi values in PESTPP-IES workflows are the summaries of objective function which will be used to terminate the workflows if the phi deference is lower than a preset threshold. It's also a measure to quantify overall match of the inversion posteriors to experimental measurements. At 10 iterations, the phi value for inversion workflow with FNO surrogates is 3.1823 which is only 1.0% larger than phi value from inversion workflow with PFLOTRAN, while achieving a 34.5% reduction on time cost. With iterations increasing from 10 to 15, the accuracy of both workflows improve with increasing time cost. At 15 iterations, the time cost reduction of FNO surrogates based inversion workflow shrinks to 28.1%.

Table 4: Summary of the two proposed PESTPP-IES inversion workflows.

iterations	PFLOTRAN workflow		FNO Surrogates workflow	
	best phi	time (min)	best phi	time (min)
10	3.1499	69.8	3.1823	45.7
15	3.0290	92.8	3.1113	66.7

After integration of these FNO surrogates into the PESTPP-IES workflow, the time efficiency of the inversion workflow has only improved 34.5% which inspires a further analysis on the time cost for the two inversion workflows. A PESTPP-IES inversion workflow includes processing template files, calling forward run commands, and processing instruction files, while the time cost of calling forward run commands is highest. The steps of processing template files and instruction files in one forward run of the two proposed inversion workflows will take 0.002 and 0.004 seconds, respectively on our devices. Calling forward run commands can be further divided into communication and simulation/prediction. In PFLOTRAN inversion workflow, the communication time cost is 0.05 seconds which is negligible compared to high computational time cost (4.04 seconds) of PFLOTRAN simulations. However, the communication time cost (2.60 seconds) is dominant in FNO surrogates inversion workflow while FNO surrogates only require 0.18 seconds to give predictions. In the above random selection of two forward runs for the two inversion workflows, the FNO surrogates workflow accumulatively will cut time cost by 32.0% compared to PFLOTRAN workflow which aligns with results from **Table 4**. It is speculated that the speed up of FNO surrogates can be significantly increased for inversion tasks with larger or finer grids when the PFLOTRAN simulations are slow and the inference speed of FNO surrogates is almost unchanged.

To visualize the inversion results from two proposed PESTPP-IES workflows, the posterior realizations with 10 iterations of the two workflows against the experimental measurements are given.

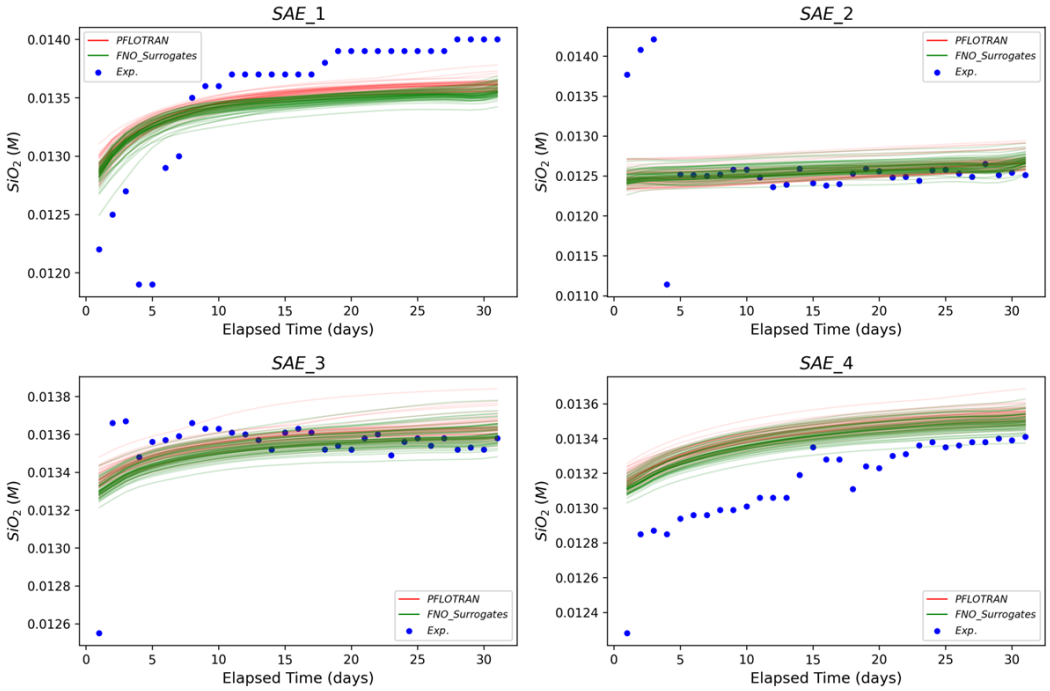

Figure 5: Comparison of realizations from two proposed workflows of SiO_2 concentration against experiments (*M: mol/L*)

Figure 5 visualizes the inversion results for silica concentration over the duration of the laboratory experiments. For SAE_1 experiment, the inversion workflow with PFLOTRAN is slightly better and the results for SAE_2 are very close. However, for SAE_3-4, the inversion workflow with FNO surrogates are showing slight advantages compared to the PFLOTRAN inversion workflow as more realizations from FNO surrogates workflow are overlapping or close to experimental results.

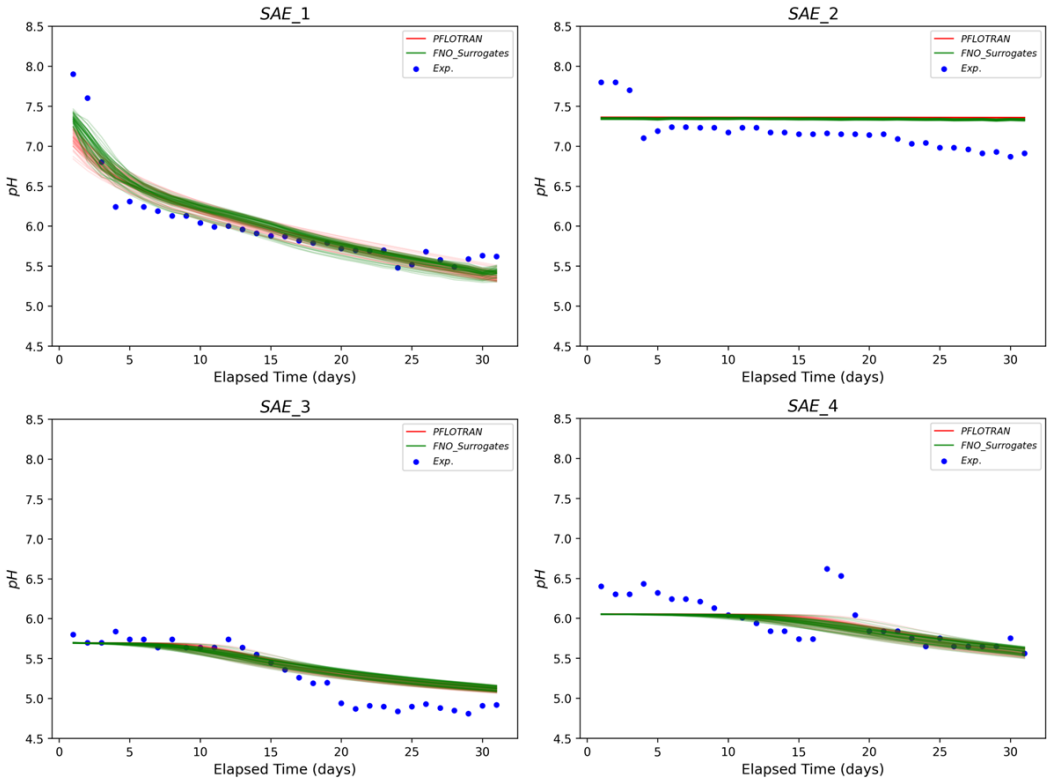

Figure 6: Comparison of realizations from two proposed workflows of pH against experiments

In **Figure 6**, the inversion results for pH values over the duration of the laboratory experiments are given. For all SAE experiments, the results from two inversion workflows are very close and both capture the distinct trends in each experiment.

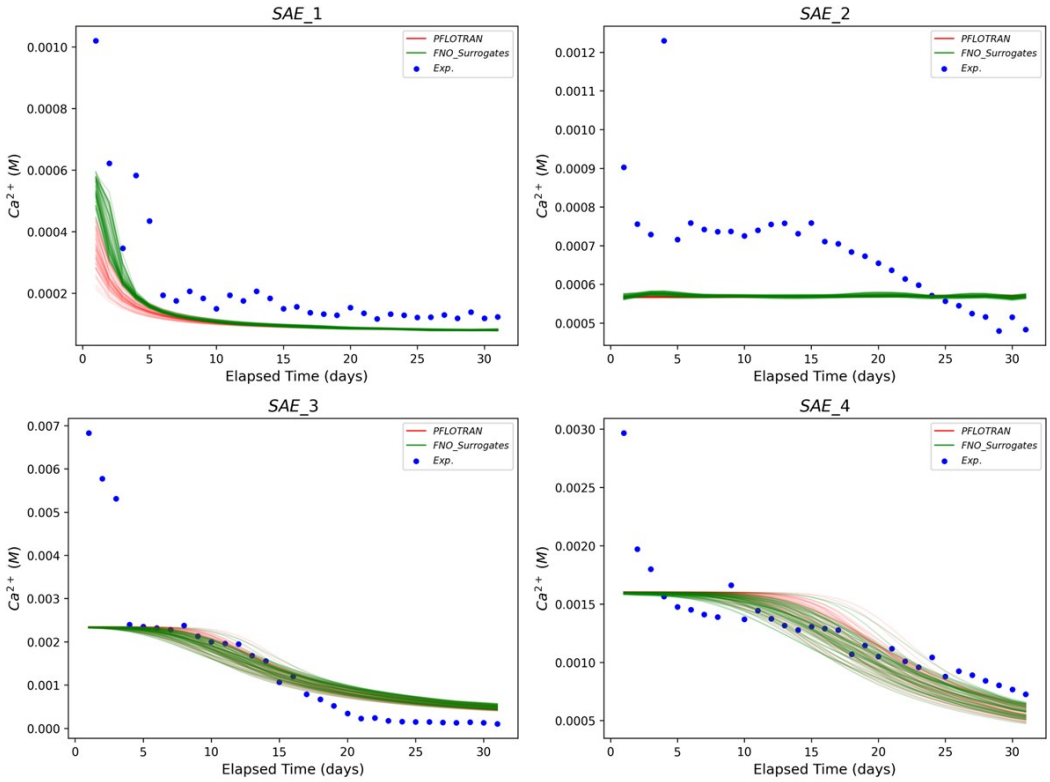

Figure 7: Comparison of realizations from two proposed workflows of Ca^{2+} concentration against experiments (*M: mol/L*)

As shown in **Figure 7**, the inversion results for Ca^{2+} concentration are very similar to the pH results from SAE_1-4. For all SAE experiments, the results from two inversion workflows are very close, and the overall trends of Ca^{2+} concentration are reproduced.

4. CONCLUSIONS

In this paper, FNO surrogates are employed to model CO_2 reinjection with produced brine and then integrated into the PESTPP-IES inversion workflow to estimate geochemical parameters. The following conclusions are drawn from this investigation.

The FNO surrogates can accurately model the temporal evolution of effluent silica concentration, pH, and Ca^{2+} concentration associated with CO_2 reinjection with produced brine in a geothermal experimental context.

The integration of FNO surrogates in PESTPP-IES will reduce the time cost by 34.5% compared to the original workflow, while maintaining the same level of accuracy. This speed up is expected to increase if a larger or finer numerical model is used: the FNO surrogate inference time will only slightly increase with model size, whereas the reactive transport model in PFLOTRAN will take significantly more time for each simulation.

Future work will focus on extending the FNO surrogates modeling to higher dimensions or field scales.

REFERENCES

Hirtz, P.V.: Silica scale control in geothermal plants—Historical perspective and current technology, Geothermal Power Generation, Woodhead Publishing, (2016), 443-476.

Daniela, B., Heuvel, V.D., Gunnlaugsson, E., Gunnarsson, I., Stawski, T.M., Peacock, C.L., Benning, L.G.: Understanding amorphous silica scaling under well-constrained conditions inside geothermal pipelines, Geothermics, 76, (2018), 231-241.

Hassani, K., and Zheng, W.: A review of recent advances in mineral scaling in geothermal energy systems: mechanisms, mitigation, and case studies, Environmental Earth Sciences, 84, 14, (2025), 418.

Byrne, D.J., Patterson, J.W., Rendel, P.M., and Mountain, B.W.: The effect of CO_2 reinjection on silica scaling in geothermal reservoirs, Proceedings, New Zealand Geothermal Workshop, Rotorua, New Zealand, (2023).

Wang, G., Liu, G., Zhao, Z., Liu, Y., & Pu, H.: A robust numerical method for modeling multiple wells in city-scale geothermal field based on simplified one-dimensional well model, Renewable Energy, 139, (2019), 873-894.

Li, Z., Kovachki, N., Azizzadenesheli, K., Liu, B., Bhattacharya, K., Stuart, A., and Anandkumar, A.: Fourier neural operator for parametric partial differential equations, arXiv preprint, (2020), arXiv:2010.08895.

Wen, G., Li, Z., Long, Q., Azizzadenesheli, K., Anandkumar, A., and Benson, S.M.: Real-time high-resolution CO_2 geological storage prediction using nested Fourier neural operators, Energy & Environmental Science, 16, 4, (2023), 1732-1741.

Tang, H., Kong, Q., and Morris, J.P.: Multi-fidelity Fourier neural operator for fast modeling of large-scale geological carbon storage, Journal of Hydrology, 629, (2024), 130641.

Guo, Q., He, Y., Liu, M., Zhao, Y., Liu, Y., and Luo, J.: Reduced geostatistical approach with a Fourier neural operator surrogate model for inverse modeling of hydraulic tomography, Water Resources Research, 60.6, (2024), e2023WR034939.

Palandri, J.L., and Kharaka, Y.K.: A compilation of rate parameters of water-mineral interaction kinetics for application to geochemical modeling, US Geological Survey, (2004), No. 2004-1068.

White, J.T.: A model-independent iterative ensemble smoother for efficient history-matching and uncertainty quantification in very high dimensions, Environmental Modelling & Software, 109, (2018), 191-201.

Chen, Y., and Oliver, D.S.: Levenberg–Marquardt forms of the iterative ensemble smoother for efficient history matching and uncertainty quantification, Computational Geosciences, 17, 4, (2013), 689-703.